npj | Climate and Atmospheric Science

www.nature.com/npjclimatsci

ARTICLE OPEN

Global urban climatology: a meta-analysis of air temperature trends (1960–2009)

Alvin C. G. Varquez[1] and Manabu Kanda[1]

Air temperature trends (1960–2009) based on stations in cities, minus those based on global surface temperature datasets, are defined herein as urban heat island (UHI) trends. Urban climate was examined globally by comparing UHI trends with indices of geophysical factors, including background climate, latitude, and diurnal temperature range (DTR) and indices of artificial factors, including anthropogenic heat emission (AHE) and population indices. Surprisingly, a better relationship was found between UHI trends and DTR—an integrated geophysical index representing thermal inertia—than with the indices of artificial factors. Thus, while an increase in sensible heat (mechanism 1) triggers UHI formation, this study infers that large thermal inertia (mechanism 2) contributes significantly on UHI. The correlation of UHI trends with other indices can be explained by both mechanisms.

npj Climate and Atmospheric Science (2018)1:32 ; doi:10.1038/s41612-018-0042-8

INTRODUCTION

Local climate modifications caused by urbanisation and global climate change can lead to unfavourable environmental conditions such as poor air ventilation, urban warming, flash floods, and health-related issues such as heat stroke and water/air-borne diseases. Health risks due to urban climates are expected to increase, especially in developing cities experiencing rapid population growth. In the recent Intergovernmental Panel on Climate Change Fifth Assessment Report, it was predicted that an increasing percentage of the world's population will be exposed to the direct impacts of climate change in urban areas. A recent study found the accumulated total costs resulting from the impact of global and local climate change on all cities since 2000 were about 2.6 times the costs without urban-weather-related effects.[1] It is therefore necessary to separate and quantify the effects of urbanisation and global climate change on warming in cities and explain differences in the mechanisms underlying the two factors. Unfortunately, there is a wide gap between urban climate and global climate change studies.

The consensus among climate change researchers is that urban areas have little influence on global warming.[2,3] In estimating global surface temperature (GST) anomalies and trends, temperatures observed in urban areas are considered outliers and not representative of the wider region, such as a spatial scale of ~100 km.[4–8] To estimate regionally representative trends, station observations in urban areas should be filtered out or adjusted.

The urban heat island (UHI) is a widely used concept that quantifies warming in a city relative to its pre-urban condition, commonly represented by its rural surroundings.[9] The UHIs have been investigated in many cities around the world.[9–14] Despite progress in UHI research in recent years, our understanding of UHIs is still limited to the regional scale. In particular, studies that can quantify factors that influence UHI formation across time and space are needed. A few studies have attempted to investigate UHIs across multiple cities simultaneously,[15–18] but there is still a need for intercontinental comparisons of UHIs and their dependence on geographical factors such as background climate, and artificial factors such as anthropogenic heating, on a global scale. Example of studies which quantified factors affecting the UHI was a recent study by Zhao et al.,[19] where contribution of physical processes or biophysical drivers to UHI intensities under present and future heat wave events were estimated using model results for cities in the United States. More research providing comprehensive interpretations from observations, in addition to models, would provide useful insights into these factors and would advance our understanding of "Global Urban Climatology".

The objectives of this study were two-fold: to separate UHIs from global climate change by extracting the temperature trends observed at urban stations from those estimated by GST, and to examine urban climate at the global scale by comparing UHI trends to geographical and artificial indicators. To achieve the second objective, which was the underlying motivation for this study, it is necessary to briefly summarise the two mechanisms behind the formation of an UHI.

RESULTS AND DISCUSSION

Generalised mechanisms for the UHI

Based on past studies of urban climate,[12,20,21] the formation of UHIs can generally be attributed to two interrelated physical mechanisms. The first and most common mechanism (mechanism 1) arises from increased sensible heat flux in urban areas caused by reductions in evapotranspiration, enhancement of heat transport by turbulence, and increases in anthropogenic heat emissions (AHEs). Neglecting other influential mechanisms (e.g., horizontal wind advection), an overall increase in the sensible heat flux correspondingly increases the air temperature throughout the day.

Conceptually known, but less well investigated, the second mechanism (mechanism 2) is the increased thermal inertia of urban surfaces.[22–26] Thermal inertia is the degree of delay in the temperature of an object matching that of its surroundings.[27]

[1]Department of Transdisciplinary Science and Engineering, Tokyo Institute of Technology, Tokyo, Japan
Correspondence: Alvin C. G. Varquez (varquez.a.aa@m.titech.ac.jp)

Received: 14 November 2017 Revised: 3 July 2018 Accepted: 8 August 2018
Published online: 25 September 2018

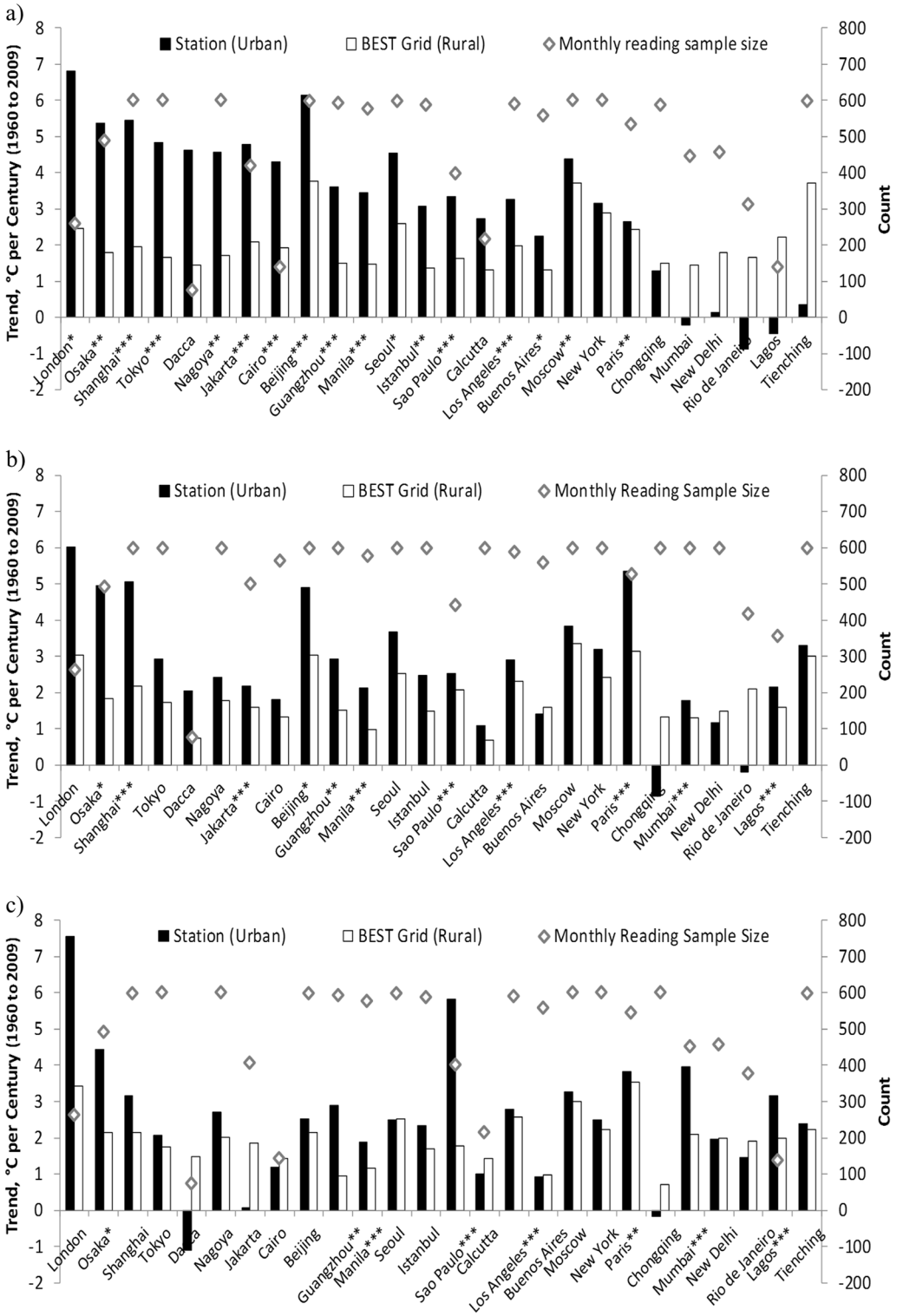

Fig. 1 Station and Berkeley Earth Surface Temperature (BEST) dataset grid trends estimated from **a** T_{min}, **b** T_{avg}, and **c** T_{max} for the largest global cities in 2010[18]. The sample size of monthly readings is indicated by the diamonds. Filled bars (unfilled bars) represent estimated trends (1960–2009) in the monthly minimum temperatures observed at each station (grid encompassing the station estimated in BEST). Representative city stations were selected based on the availability of monthly data. The number of asterisks beside a city's name denotes the *p*-values of the estimated trends at the stations (*, **, and *** correspond to $p < 0.15$, 0.10, and 0.05, respectively)

Urban surfaces are three-dimensional in nature, with relatively large heat storage capacities. Moreover, their complex geometry enhances heat entrapment by multi-reflection of solar and infrared radiation from the walls of street canyons. This trapping of heat results in higher resistance to temperature changes, i.e., higher thermal inertia, than that of surrounding non-urban surfaces. During the day, incoming solar radiation is trapped within street canyons and the reduced amounts of sensible heat

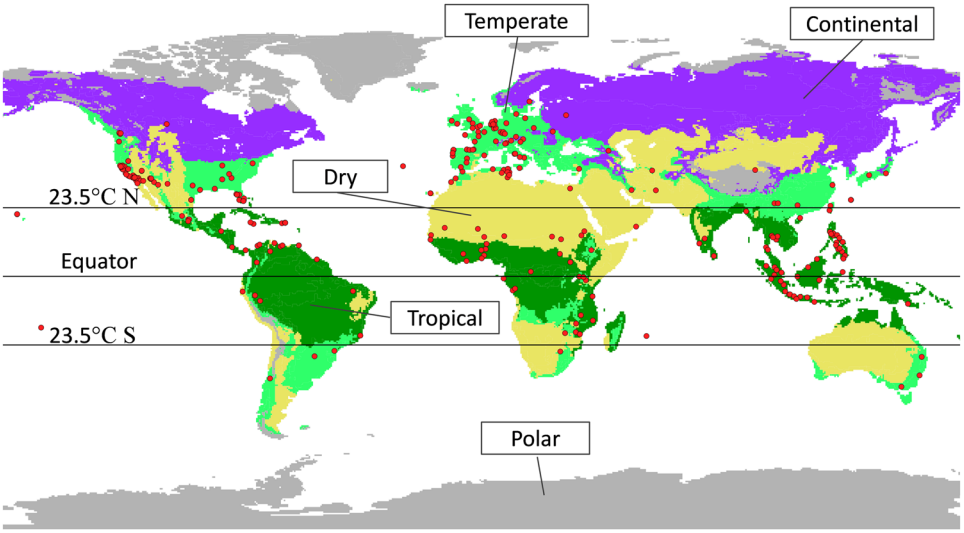

Fig. 2 Filtered stations (286) from the quality-controlled Berkeley Earth Surface Temperature dataset (BEST) (red points). Filtering was conducted by considering statistical significance and the number of monthly data samples per station (see Supplementary Methods for selection criteria)

can result in cooler daytime temperatures than those over flat surfaces. During the night, outgoing infra-red radiation is restricted within street canyons, and the release of surplus heat that was stored during the day results in higher nighttime temperatures than in surrounding areas, where temperatures drop due to radiative cooling. In effect, the thermal inertia of urban surfaces influences the diurnal temperature range (DTR) near those surfaces, such that a higher thermal inertia results in a smaller DTR. This mechanism explains the occasionally observed daytime negative UHI, the so-called urban cool island, and the commonly observed positive nighttime UHI, i.e., nocturnal UHI.

In an urban environment, both mechanisms are expected to influence the UHI. The background climate of a city provides the baseline values of sensible heat and thermal inertia in its pre-urban (or rural) condition. This implies that the extent of an UHI will depend on the background climate (or geophysical indicators) in addition to the level of urbanisation (or artificial indicators). The two mechanisms—increased sensible heat and larger thermal inertia—will be used to explain the relationship of UHIs to geophysical/artificial indicators in the latter discussions.

UHI trend comparisons for large cities

Temperature observations (source and intermediate Berkeley Earth Surface Temperature dataset[8] [BEST]) closest to the centres of the largest agglomerations,[28] with monthly statistics available from January 1960 to December 2009 (covering 40 years), were analysed. The calendar months are represented by the year and decimal fraction of a year corresponding to the midpoint of the time period being represented.[8] Of 30 cities, only 26 were considered due to the lack of available records for the other 4 cities (Mexico City, Karachi, Shenzhen, and Kinshasa). Figure 1 shows a comparison of the temperature trends calculated from station observations and the corresponding grid derived from the monthly statistics, T_{min}, T_{max}, and T_{avg}. The cities are arranged according to the largest positive differences between trends in T_{min}. A two-sided *p*-value was also calculated (denoted by asterisks), where the null hypothesis was that the slope is zero, to evaluate the reliability of the estimated trends, in addition to the sample count (secondary axis).

Most of these large cities exhibited positive UHI trends, with mean UHI trends of 1.12 ± 2.08 and 0.53 ± 1.47 °C/century for nighttime and daytime values, respectively. The values varied substantially from one city to another, as indicated by the large sample standard deviations compared with the means. As in previous studies,[29,30] nighttime UHI trends tended to be larger than the daytime UHI trends; there were more samples that displayed statistically significant trends (from *p*-values) in nighttime estimates than in daytime estimates. The reasons for these differences will be discussed later. Furthermore, the statistics changed substantially when cities with a higher statistical significance (labelled with three asterisks in Fig. 1a) were used; the mean UHI trends increased to 2.36 ± 0.69 and 1.60 ± 1.50 °C/century for nighttime and daytime values, respectively. This implies that further statistical tests and screening are required prior to application of this approach to the full BEST dataset. The screening process is summarised in the Supplementary Methods. After screening, 286 city samples were acquired and were used in the work described in the following discussions (Fig. 2).

Urban vs. rural air temperature trends

Figure 3 shows box plots and histograms of the trends derived from the urban stations and from the BEST grid assumed to represent adjacent rural areas. The mean daily average UHI trend was 1.38 °C/century (Fig. 3c). A similar tendency was found to that in the previous analysis, in which nighttime UHI trends (2.50 °C/century) were significantly larger than daytime UHI trends (0.22 °C/century). The spread of the urban trends far exceeded that of the surrounding rural areas (i.e., urban trends had an interquartile range twice that of the rural trends). The trend in rural areas immediately surrounding urban areas was limited to within 0–4 °C/century.

False discovery rate approach was conducted for the trends calculated from the selected 286 stations. Kendall's Tau was estimated and "field significance" was assessed by controlling the false detection rate (see SI for the result) at 5% significance. The result shows that there is 97.9%, 97.2%, 44.8% of false positives from the trends of T_{min}, T_{avg}, and T_{max} from the urban stations, respectively. This suggests that the trends estimated for T_{min} and T_{avg} were mostly statistically significant, whereas that of T_{max} suggests statistically insignificant trends. Except for the trends of T_{max} since their lack in statistical significance in most stations can also be interpreted physically that trends were not apparent during daytime, the rest of the analyses for T_{min} and T_{avg} only focuses on significant trend estimates.

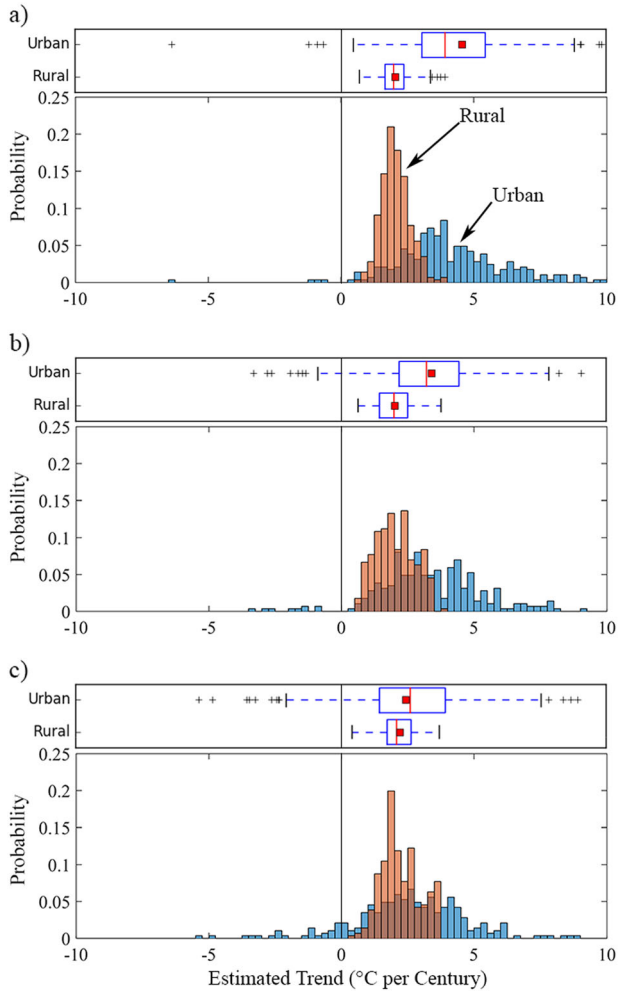

Fig. 3 Histograms of air temperature trends at urban stations and rural areas, represented by BEST dataset grids. The horizontal axis is bounded by the actual range of the trend estimated from **a** T_{min}, **b** T_{avg}, and **c** T_{max}. The histogram bar interval is 0.25 °C; 286 stations were used

UHI trends in relation with geophysical and artificial indicators

The relations between UHI trends and several geophysical and artificial indicators, available at a global scale, were investigated. We focused on the indicators that we found most relevant to the UHI trends after testing multiple datasets available at the global scale. The geophysical indicators were climate regime, latitude, DTR, background wind speed, vegetation cover, and distance from the nearest coastline, while artificial indicators were AHE and population. Artificial indicators refer to parameters directly induced by humans. The preparation of these indicators is summarised in the Supplementary Notes.

Geophysical indicator: climate regime

Figure 4 shows box plots of UHI trends grouped by climate zones according to the main Köppen–Geiger climate sub-classes[31] (Fig. 2). Cities with dry climates tended to have the largest nighttime UHI trend values (Fig. 4a), followed by cities in continental and temperate climate zones. Tropical cities had the smallest UHI trends, with several being negative. Daily average UHI trends (Fig. 4b) were similar to nighttime UHI trends, except that the intensities were smaller. Compared to nighttime and daily average trends, the daytime UHI trends (Fig. 4c) were the smallest in all climate zones, with almost half of all stations having negative trend values. In addition, cities in continental climates had the largest daytime UHI trends. Mechanisms 1 and 2 were apparent in cities in continental and dry climates, respectively. Continental climate zones tended to have more positive urban–rural sensible heat differences that were apparent throughout the day. On the other hand, large thermal inertia differences in urban–rural deserts caused significantly positive nighttime UHI trends, and smaller, sometimes negative, daytime UHI trends. Care must be taken with the statistics in the continental climate zones because of its lack in samples.

Geophysical indicator: latitude

In agreement with previous climate change studies,[32] a tendency for temperature trends to increase at higher latitudes was found (grey line denoting rural areas in Fig. 5a, b, c). The UHI trends, except in the daytime, of the urban stations also increased with latitude, except in dry climates at mid-latitudes (red markers in Fig. 5a, b, c). Mechanism 1 may explain the general increase in UHI trends with increasing latitude, with cities located far from the equator generally having much lower background (rural) sensible heat fluxes, due to the limited amount of incoming solar radiation. As rural or background temperature trends increased with latitude as a result of global climate change, the temperature trends in urban areas likewise increased and were generally larger than those of their rural counterparts due to urbanisation. On the other hand, mechanism 2 may explain the large UHI trends at mid-latitudes because in dry regions the background thermal inertia is much lower in rural locations.

Geophysical indicator: DTR

DTR was found to be adequately related to the urban trends (Fig. 5d–f). Urbanisation increases the thermal inertia (i.e., DTR decrease) in cities, as explained earlier (mechanism 2). This is why the nighttime and daily average UHI trends increased with increasing DTR (Figs. 5d, e, 6a), while the daytime UHI trends decreased (Fig. 5f). The decrease in DTR was both indirectly and directly caused by increased transport by turbulence (see earlier discussion) and increased heat capacity (thermal inertia), respectively. Heat capacity depends on the physical properties of a surface material, among which wetness is the most influential factor. The larger UHI trends in dry regions and smaller UHI trends in tropical regions (Fig. 4) can be explained by differences in wetness (e.g., precipitation), which affect the background (initial) DTR. Despite the differences in approach, the current logic agrees with an earlier study[17] that focused on US cities, which found that UHIs are negatively correlated with precipitation amounts in regions with a high occurrence of precipitation, e.g., tropical regions.

Geophysical indicator: background wind speed

The decrease in UHI trends with increasing wind speed varied among climate regimes; dry regions experienced the largest decrease (red lines in Fig. 6b) followed by temperate regions (blue lines in Fig. 6b). UHI trends in tropical regions were insensitive to wind speed (Fig. 6b). The dependency of UHI trends on wind speed can be explained by mechanism 2 (thermal inertia). Stronger wind speeds activate turbulent heat transport between the surface and the atmosphere above. This decreases the amount of heat being trapped within the surface layer, thereby reducing background daytime temperatures. In a study by Sun et al.,[33] the same conclusion was reached that enhanced wind speeds during heat wave conditions in four temperate cities tend to reduce the heat storage. Strong wind speeds also tend to increase background nighttime temperatures as warm air from urban areas is advected to its surroundings.[34] This results in an indirect decrease in the background (rural) DTR. Tropical regions generally have a

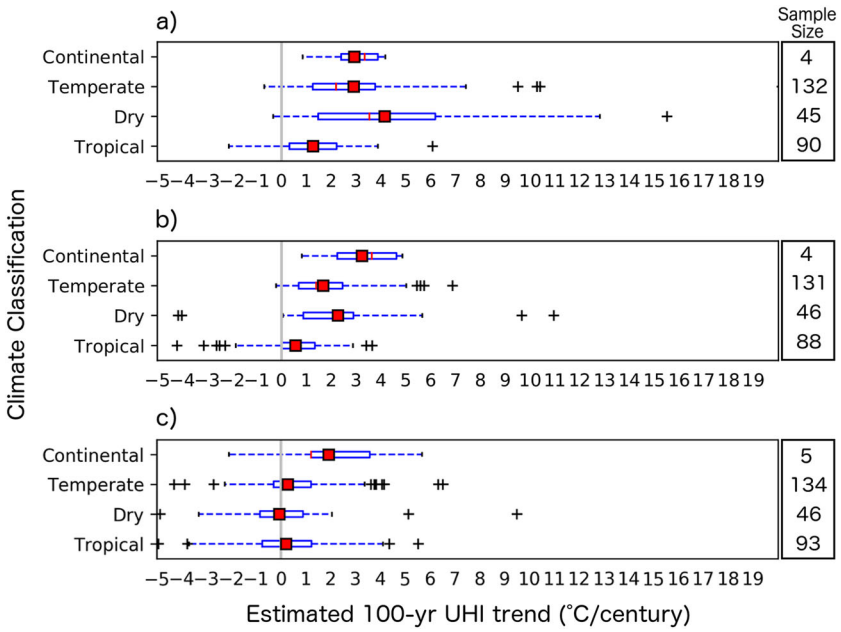

Fig. 4 Urban heat island (UHI) trends from stations grouped by climate classification (Köppen–Geiger). Estimated from **a** T_{min}, **b** T_{avg}, and **c** T_{max} with 286 total samples. False discovery rate approach was applied except for **c** (see text and Supplementary Notes)

lower DTR than other regions; thus, in such regions, DTR reduction by increasing wind speed is negligible. During heat wave conditions,[33] areas where wind speeds were already low would result to no changes or even reductions to the heat storage.

Geophysical indicator: vegetation cover

Although the UHI trends decreased with increasing vegetation cover overall (Fig. 6c), a wide scatter was found for low-vegetation areas (i.e., vegetation cover <40%). When vegetation covers more than 40% of the land, more of the incoming radiation is returned to the atmosphere as latent heat via transpiration than is returned as sensible heat. This effect of vegetation to mitigate UHIs is well known,[35] but its effect on UHI trends was confirmed in this study, although scatter is still apparent. At low-vegetation areas, the background climate and other land cover types become more influential.

Artificial indicator: AHEs

AHE is a widely known[25] driver of UHIs that modifies the sensible heat flux in cities (mechanism 1). It is obvious from Fig. 6d that compared with the geographical indicators discussed previously, AHE is not a strong indicator of UHI trends globally. If the study were conducted on a smaller scale, where differences in background climate are negligible, the relationship between UHI trends and AHE might be more obvious, because areas with large UHI intensities are influenced by large AHE.[36–39] However, this was not the case when distant cities with different background climates were compared (e.g., cities in tropical regions with cities in humid regions) due in part to the more dominant influence of mechanism 2 (differences in thermal inertia).

Artificial indicator: population and distance to the nearest coastline

As with the other indicators investigated, but excluded in the discussion, population and the distance between urban stations and the nearest coastline (see Supplementary Fig. 3) were not related to UHI trends at the global scale.

SUMMARY OF RESULTS

The numbers of studies of climate change and of urban climate have been increasing in recent decades, but a wide gap remains between the two fields. Climate change has been investigated at coarse spatial and temporal resolutions, leading to a lack of consideration of urbanisation. On the other hand, urban climate studies have focused mainly on specific cities and have not provided inter-comparisons of UHIs at the global scale. To overcome the gap between these fields of study, a UHI-trend estimation method that can be applied to all available urban stations around the world is proposed. After evaluating the UHI trends for the largest cities in the world, the mechanisms behind UHI formation were investigated by comparing the estimated trends with geophysical and artificial indices. There are two general mechanisms for UHI formation. The first and most widely known is the increase in sensible heat in urban areas, while the second results from the increase in thermal inertia in urban areas. The findings of this first global evaluation of UHI trends spanning the period of January 1960 to December 2009 can be summarised as follows:

a. The mean UHI trends of 286 urban stations around the world with a range of background climates were mostly positive and found to be largest at night (2.36 ± 0.69 °C/century) and smallest during the day (1.60 ± 1.50 °C/century).
b. The UHI trend was found to increase with latitude, except at mid-latitudes. The decrease in solar radiation and resulting reduction in sensible heat at higher latitudes were more sensitive to increased urban sensible heat flux (mechanism 1). The large scatter of UHI trend values in mid-latitude regions was due to differences in background thermal inertia (mechanism 2).
c. UHI trends increased with increasing DTR. DTR, an integrated geophysical index representing thermal inertia (mechanism 2), was found to be a comprehensive indicator for UHIs. The UHI trend in each background climate was strongly linked with the DTR, such that dry (tropical) climates tended to have a higher (lower) DTR and, likewise, a larger (smaller) UHI trend.
d. Stronger winds tended to reduce nighttime UHI trends. High wind speeds reduce thermal inertia as a result of enhanced

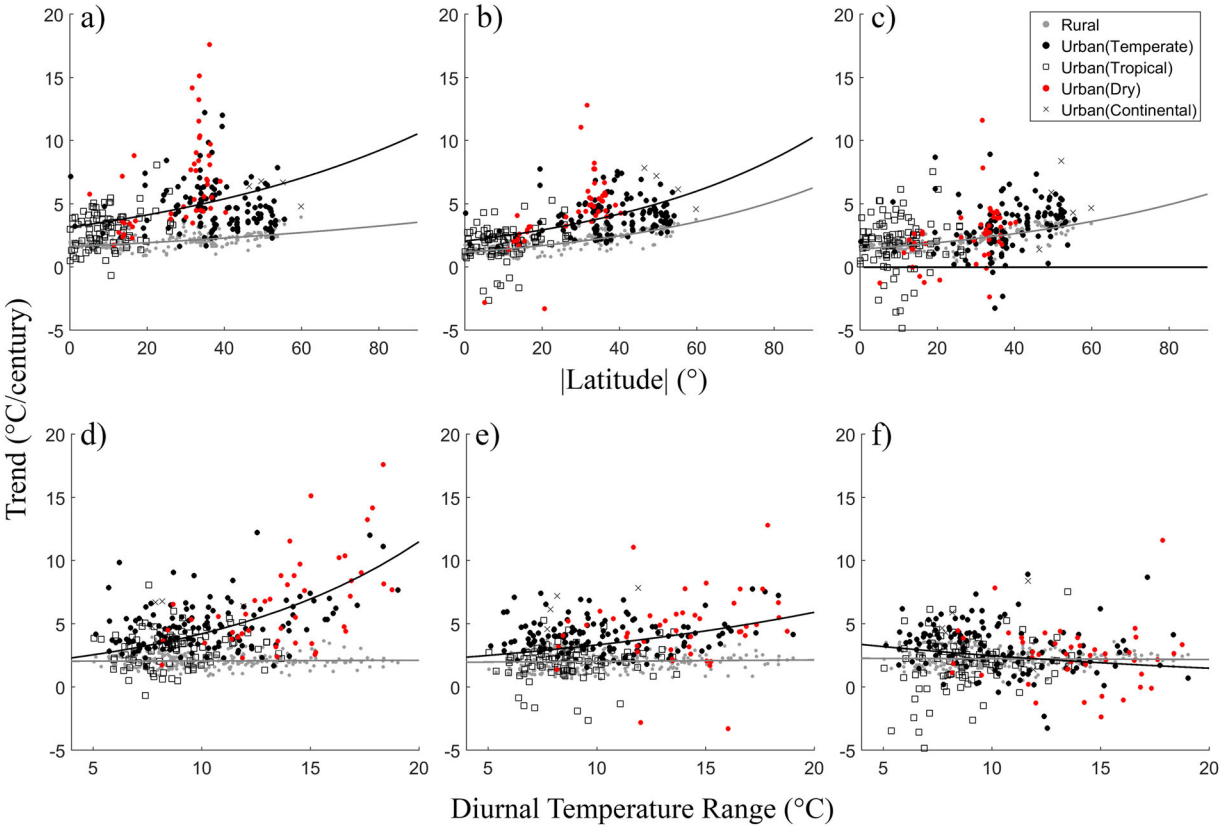

Fig. 5 UHI trend dependence on latitude for **a** T_{min}, **b** T_{avg}, and **c** T_{max}; UHI trend dependence on the diurnal temperature range (DTR) for **d** T_{min}, **e** T_{avg}, and **f** T_{max} for both urban and rural stations. Black and grey lines represent quadratic regressions (only as guide) of the urban and rural trends, respectively; 286 stations were used. False discovery rate approach was applied except for **c** and **f** (see text and Supplementary Notes)

heat transport through turbulence. This relationship is more significant in a dry climate, with a high DTR, than in a tropical climate, with a low DTR (mechanism 2).

e. The UHI trend was negatively correlated with vegetation cover. This relationship was more apparent with relatively high levels of vegetation cover, which result in more incoming radiation being converted to latent heat via transpiration than is present as sensible heat. The large scatter of UHI trends in areas with low vegetation cover was due to the differences in background thermal inertia (mechanism 2).
f. Indices of artificial factors such as AHE and population (more strongly related to mechanism 1) were found to have an insignificant correlation with the UHI trend. This means that at the global scale, artificial indices were less indicative of the UHI trend than were geographical indices such as DTR.

Another method to investigate the UHIs of multiple cities is the use of land surface temperatures (LSTs) measured by remote sensing.[36] However, using LSTs for UHI studies has many shortcomings compared with the use of trends from near-surface air temperature stations. First, the physical representation of satellite-estimated LSTs is uncertain for very rough and spatially heterogeneous environments.[37] Second, LSTs are more sensitive to spatial and temporal changes in surface conditions than air temperatures,[38] which under certain atmospheric conditions LSTs could fluctuate erratically. The use of long-term trends, such as those used in this study, minimises the effects of this fluctuation. Third, diurnal and long-term LST measurements are currently limited or unavailable. Finally, the mechanisms that affect LSTs cannot be directly applied to air temperatures due to their physical differences.

For all comparisons between the UHI trend and the indicators, wide scatter remains because all indicators are actually influencing or influenced by each other in the real environment. Deeper investigations which can consider these interactions are needed. Due to the simplicity and uniqueness of our proposed methodology for estimating the UHI trends, we recommend that the current findings should be confirmed using alternative GST datasets other than the BEST. Moreover, the use of simple linear regression, a common approach to estimate trends in climate change studies, needs further verification.

Finally, population was mainly used to identify urban stations in this study. Few urban stations show large vegetation fractions (Fig. 6c), which could possibly be caused by the inherent uncertainty in the vegetation dataset. Nevertheless, the vegetation fraction dataset is accurate as a relative measure of how vegetated the surroundings of the stations. A more standard definition of an urban area and the consistency of global datasets to be used in future similar studies is needed.

METHODS

UHI estimation by long-term temperature records (UHI trends)

UHI is generally estimated from the spatial difference between urban and rural temperatures. However, in this study, UHIs were estimated using the trends of long-term temperature records.[15] Unlike the former approach, the latter approach tends to minimise the issue of the spatial representativeness of temperatures observed in cities. The complex surface nature of urban areas gives rise to spatially inhomogeneous temperature distributions, with surface temperatures varying several degrees more than air temperatures. This means that spatial estimations of UHIs based on either remote sensing or station observations have limitations. On the other hand, the trade-off of using trends to estimate UHIs is that careful

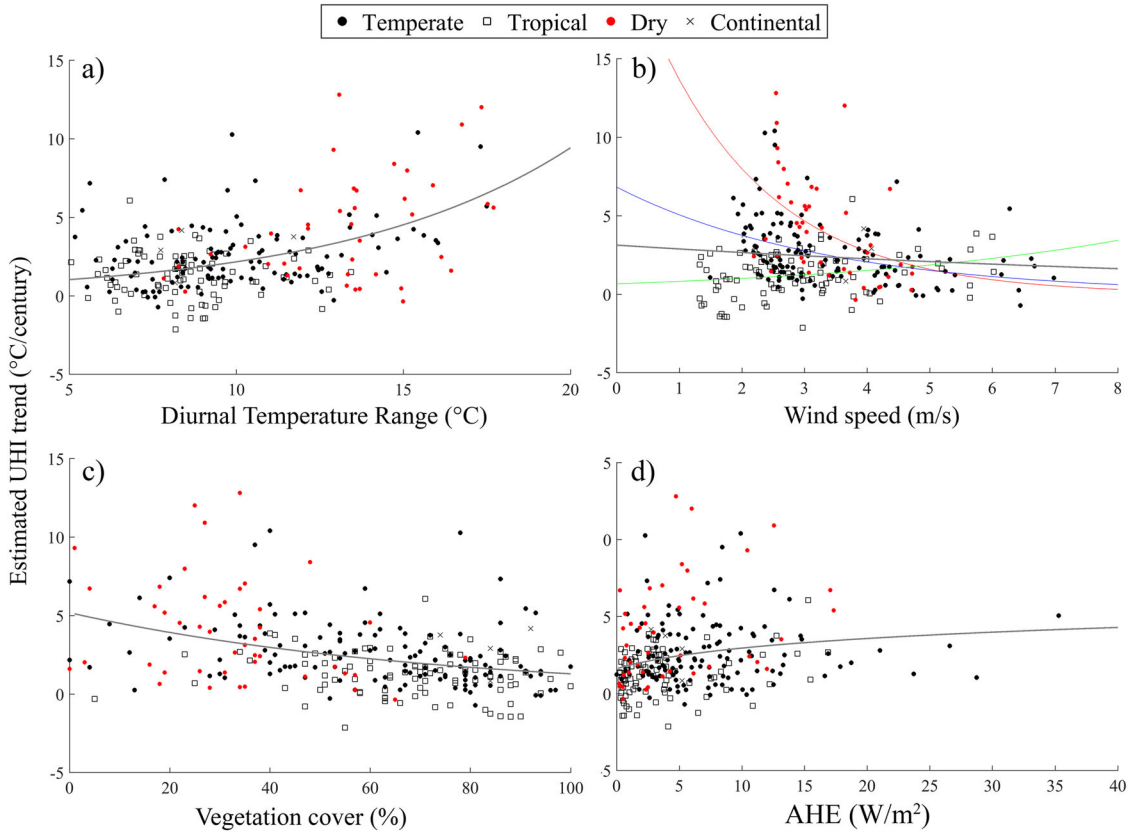

Fig. 6 Comparisons between nighttime UHI trends and **a** DTR, **b** wind speeds, **c** vegetation cover, and **d** anthropogenic heating. Stations were grouped into Köppen–Geiger climate zones. Black lines are regression curves (only as a guide) using all of the analysed stations. The red, blue, and green lines in **b** are regressions for cities in dry, temperate, and tropical zones, respectively; 286 stations were used. False discovery rate approach was applied (see text and Supplementary Notes)

inspection of the quality of available long-term records is necessary. Fortunately, the quality of the long-term records used in the construction of existing GSTs has already been verified in the GST datasets.

The process of estimating UHIs based on the Berkeley Earth Surface Temperature (BEST) dataset,[8] a GST dataset, will be briefly summarised. Temperature trends for the target period were estimated based on quality-controlled data from stations located in urbanised areas and corresponding gridded data that were assumed to represent surrounding rural areas. The assumption that BEST grids correspond to rural areas derives from the estimation of BEST, in which readings from urban stations were given a lesser weighting in the averaging than those from rural stations.[8] Trends (°C/century) were estimated from the slope of the linear regression between monthly statistical values (i.e., means of daily minimum, maximum, and average) and their corresponding months in yearly fraction units. UHI trends were acquired by subtracting the trend estimated for an urban station from that estimated for its immediate rural area (grid). Specific details are discussed in the Supplementary Methods. From the common assumption[40] that mean monthly statistics of daily T_{min} and T_{max} correspond to monthly means of peak nighttime and daytime temperature values, respectively, the nighttime, daytime, and daily average UHI trends were calculated from the UHI trends estimated from T_{min}, T_{max}, and T_{avg}, respectively.

DATA AVAILABILITY

The fully processed datasets containing the trends are available from the corresponding author upon request. The source of all datasets used to estimate the indicators are mentioned in the Supplementary Notes and are obtained from their public websites.

ACKNOWLEDGEMENTS

This study was supported by the Grant-in-Aid for Scientific Research (A) 17H01292.

AUTHOR CONTRIBUTIONS

A.C.G.V. and M.K. both contributed to the completion of the manuscript through the following: (a) Substantial contributions to the conception or design of the work or the acquisition, analysis or interpretation of the data; (b) drafting the work or revising it critically for important intellectual content; (c) final approval of the completed version; (d) accountability for all aspects of the work in ensuring that questions related to the accuracy or integrity of any part of the work are appropriately investigated and resolved.

ADDITIONAL INFORMATION

Supplementary Information accompanies the paper on the *npj Climate and Atmospheric Science* website (https://doi.org/10.1038/s41612-018-0042-8).

Competing interests: The authors declare no competing interests.

Publisher's note: Springer Nature remains neutral with regard to jurisdictional claims in published maps and institutional affiliations.

REFERENCES

1. Estrada, F., Botzen, W. J. & Tol, R. S. A global economic assessment of city policies to reduce climate change impacts. *Nat. Clim. Change* **7**, 403–406 (2017).
2. Peterson, T. C. et al. Global rural temperature trends. *Geophys. Res. Lett.* **26**, 329–332 (1999).
3. Parker, D. E. Urban heat island effects on estimates of observed climate change. *Wiley Interdiscip. Rev. Clim. Change* **1**, 123–133 (2009).
4. Smith, T. M. & Reynolds, R. W. A global merged land–air–sea surface temperature reconstruction based on historical observations (1880–1997). *J. Clim.* **18**, 2021–2036 (2005).
5. Peterson, T. C., Vose, R., Schmoyer, R. & Razuvaëv, V. Global historical climatology network (GHCN) quality control of monthly temperature data. *Int. J. Climatol.* **18**, 1169–1179 (1998).

6. Jones, P. D., New, M., Parker, D. E., Martin, S. & Rigor, I. G. Surface air temperature and its changes over the past 150 years. *Rev. Geophys.* **37**, 173–199 (1999).
7. Hansen, J., Ruedy, R., Sato, M., & Lo, K. Global surface temperature change. *Rev. Geophys.* **48**, RG4004 (2010).
8. Rohde, R., Muller, R., Jacobsen, R., Perlmutter, S., & Mosher, S. Berkeley earth temperature averaging process. *Geoinfor. Geostat.: An Overview* **1**, 2 (2013).
9. Oke, T.R. Review of urban climatology 1968–1973. Technical Note. World Meteorological Organization, no. 134 (1974).
10. Peterson, J. T. in *Climate in Review* (ed McBoyle, G.) 264–285 (Houghton Mifflin, Boston, 1973).
11. Landsberg, H. E. *The Urban Climate*. 2nd edn, 28 (Elsevier Science, New York, 1981).
12. Arnfield, A. J. Two decades of urban climate research: a review of turbulence, exchanges of energy and water, and the urban heat island. *Int. J. Climatol.* **23**, 1–26 (2003).
13. Unger, J. Intra-urban relationship between surface geometry and urban heat island: review and new approach. *Clim. Res.* **27**, 253–264 (2004).
14. Roth, M. Review of urban climate research in (sub)tropical regions. *Int. J. Climatol.* **27**, 1859–1873 (2007).
15. Ajaaj, A. A., Mishra, A. K., & Khan, A. A. Urban and peri-urban precipitation and air temperature trends in mega cities of the world using multiple trend analysis methods. *Theor. Appl. Climatol.* **132**, 1–16 (2017).
16. Kalnay, E. & Cai, M. Corrigendum: impact of urbanisation and land-use change on climate. *Nature* **425**, 102–102 (2003).
17. Kataoka, K., Matsumoto, F., Ichinose, T. & Taniguchi, M. Urban warming trends in several large Asian cities over the last 100 years. *Sci. Total Environ.* **407**, 3112–3119 (2009).
18. Zhao, L., Lee, X., Smith, R. B. & Oleson, K. Strong contributions of local background climate to urban heat islands. *Nature* **511**, 216–219 (2014).
19. Zhao, L. et al. Interactions between urban heat islands and heat waves. *Environ. Res. Lett.* **13**, 034003 (2018).
20. Grimmond, C. S. B. Progress in measuring and observing the urban atmosphere. *Theor. Appl. Climatol.* **84**, 3–22 (2005).
21. Oke, T. R., Mills, G., Christen, A. & Voogt, J.A. *Urban Climates* (Cambridge University Press, Cambridge, 2017).
22. Grimmond, C. S. & Oke, T. R. Heat storage in urban areas: local-scale observations and evaluation of a simple model. *J. Appl. Meteor.* **3**, 922–940 (1999).
23. Chow, W. T. & Roth, M. Temporal dynamics of the urban heat island of Singapore. *Int. J. Climatol.* **26**, 2243–2260 (2006).
24. Kawai, T. & Kanda, M. Urban energy balance obtained from the comprehensive outdoor scale model experiment. Part I: basic features of the surface energy balance. *J. Appl. Meteorol. Clim.* **49**, 1341–1359 (2010).
25. Kanda, M. Progress in urban meteorology: a review. *J. Meteorol. Soc. Jpn.* **85B**, 363–383 (2007).
26. Ryu, Y.-H. & Baik, J.-J. Quantitative analysis of factors contributing to urban heat island intensity. *J. Appl. Meteorol. Climatol.* **51**, 842–854 (2012).
27. "thermal inertia". Merriam-Website. Merriam-Webster.com (2017).
28. United Nations, Department of Economic and Social Affairs, Population Division *World Urbanisation Prospects: The 2014 Revision, CD-ROM Edition*. https://esa.un.org/unpd/wup/CD-ROM/ (2014).
29. Karl, T. R., Kukla, G. & Gavin, J. Decreasing diurnal temperature range in the United States and Canada from 1941 through 1980. *J. Clim. Appl. Meteorol.* **23**, 1489–1504 (1984).
30. Oleson, K. W., Bonan, G. B., Feddema, J. & Vertenstein, M. An urban parameterization for a global climate model. Part II: sensitivity to input parameters and the simulated urban heat island in offline simulations. *J. Appl. Meteorol. Clim.* **47**, 1061–1076 (2008).
31. Kottek, M., Grieser, J., Beck, C., Rudolf, B. & Rubel, F. World map of the Köppen-Geiger climate classification updated. *Meteorol. Z.* **15**, 259–263 (2006).
32. Screen, J. A. & Simmonds, I. The central role of diminishing sea ice in recent Arctic temperature amplification. *Nature* **464**, 1334–1337 (2010).
33. Sun, T. et al. Attribution and mitigation of heat wave-induced urban heat storage change. *Environ. Res. Lett.* **12**, 114007 (2017).
34. Bassett, R. et al. Observations of urban heat island advection from a high-density monitoring network. *Q. J. R. Meteorol. Soc.* **142**, 2434–2441 (2016).
35. Gallo, K. P. et al. The use of a vegetation index for assessment of the urban heat island effect. *Int. J. Remote. Sens.* **14**, 2223–2230 (1993).
36. Taha, H. Urban climates and heat islands: albedo, evapotranspiration, and anthropogenic heat. *Energ. Build.* **25**, 99–103 (1997).
37. Ichinose, T., Shimodozono, K. & Hanaki, K. Impact of anthropogenic heat on urban climate in Tokyo. *Atmos. Environ.* **33**, 3897–3909 (1999).
38. Kłysik, K. & Fortuniak, K. Temporal and spatial characteristics of the urban heat island of Łódź, Poland. *Atmos. Environ.* **33**, 3885–3895 (1999).
39. Rizwan, A. M., Dennis, L. Y. C. & Liu, C. A review on the generation, determination and mitigation of urban heat island. *J. Environ. Sci.* **20**, 120–128 (2008).
40. Mccarthy, M. P., Best, M. J., & Betts, R. A. Climate change in cities due to global warming and urban effects. *Geophys. Res. Lett.* **37**, L09705 (2010).